

Combining Statistical and Graph-Based Approaches to Classification of Interstitial Pulmonary Diseases

Álvaro Albuquerque[†], Yana Mendes^{*}, Eliana Almeida[†], Raquel Cabral[†] and Fabiane Queiroz[†]

^{*}Federal Institute of Alagoas - IFAL, Brazil

[†]Federal University of Alagoas - UFAL, Brazil

Abstract—Problems of texture classification are consistently challenging once the patterns of different instances can be very similar. In the context of medical imaging, this group of methods can aid in diagnosing patients as part of the concept of Computer-Aided Diagnosis (CAD). In this paper, we propose a method for texture classification in the context of classifying Interstitial Pulmonary Diseases (IPDs) on high-resolution Computed Tomographies (CTs) using concepts of complex networks and statistical metrics. Our approach is based on mapping the input image into multiscale graphs and extracting the closeness centrality metric. We combine the feature vector resulting from the closeness analysis with Haralick and Local Binary Pattern descriptors. We analyze the proposed approach’s performance by comparing it with other methods and discussing its metrics for each class (IPD pattern) of the dataset. Based on the results, we can highlight our technique as an aid on the problem of diagnosing patients with COVID-19.

I. INTRODUCTION

Interstitial Pulmonary Diseases (IPDs), also called Diffuse Parenchymal Diseases, form a group with more than 150 different pathologies that affect the interstitial region, including walls of the air sacs of the lungs and areas around blood vessels and lower airways [1]. The patient’s complete history (symptoms, family history, disease record), physical examination, laboratory tests, pulmonary function tests, and visual findings on chest radiographs are essential in diagnosing IPDs. Computer-Aided Diagnosis (CAD) has become one of the major research subjects in medical imaging and diagnostic radiology [2]. One way to diagnose IPDs is the visual analysis of tomography (CT) images (see Figure 1). Textures present in digital images are complex visual patterns with particular characteristics and weight can see them as powerful discriminators for images. The texture classification process consists of an essential step in Medical Image Analysis tasks and their applications, including content-based medical image retrieval, classification and segmentation. According to [1], the IPD’s are diseases that have a consistently difficult process of classification. In other words, it is not trivial, because the characteristics of some texture patterns can be difficult to differentiate and easily lead to incorrect results.

One of the main challenges in texture classification is developing an efficient descriptor invariant to rotations, scale, and lighting variations. We can perform an accurate texture classification using a large number of approaches like the statistical ones (e.g., gray level co-occurrence matrix (GLCM)), Local Binary Patterns (LBP), graph-based approaches with

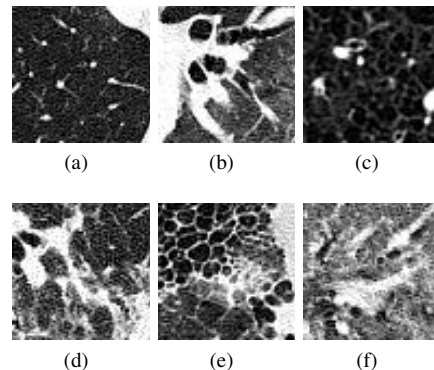


Fig. 1. ROIs presenting texture patterns of IPDs in high-resolution CT images: (a) Healthy Lung (b) Pulmonary Consolidation (c) Emphysematous Area (d) Septal Thickening (e) Honeycomb (f) Ground-glass Opacity.

touristic walkers [3] and shortest path in graphs [4], learning-based approaches [5], etc.

Complex Networks (CNs) are irregular and comprehensive structures inspired by empirical analysis of real networks that allow us to understand various real systems [6]. We call these systems “complex systems” because it is not possible to predict their collective behavior from their single components. But understanding the topological description of these systems makes us capable of predicting them and possibly control them. CNs are described by several metrics, which represent their topological properties.

Here, we present a method, based on Statistical descriptors and graphs-based ones (CNs), for classifying CT images that show IPDs texture patterns.

II. RELATED WORKS

Texture descriptors extract attributes from images and represent them efficiently, providing more outstanding classification performance, regardless of the classifier used [7]. In general, Graph-based methods methodology maps the image in a network and use topological aspects of it to characterize and classify textures [8], [9].

According [8], an image is mapped to a regular directed network in which each pixel becomes a vertex that are connected if they are within a neighborhood determined by a radius value r . A thresholding operation is applied to transform the regular network into a scaled one. A set of edges are removed in this process, depending on this threshold value.

Several threshold values were used, obtaining multiple scaled networks from a single image. For each network, random walks were applied to estimate the activity in a given network. An activity values histogram was generated by the association of the *in-degree* values of the vertices with the number of steps of the walker in these same vertices. The histogram values are concatenated by varying the threshold, thus generating a vector of attributes for a given image. Another work that addresses the characterization of textures with graphs is [9]. This work presents the texture descriptor that uses deterministic walks and vertex *in-degree* values to generate a feature vector.

Global methods for texture classification describe the image as a whole to generalize a given object. Neuroscience researchers said that the human brain combines Local and Global information to recognize objects. The works of [8] and [9] are promising. Still, they present the problem of extracting texture features through only local aspects since the analysis considers only in-degree values from the network. This centrality metric represents the number of incoming edges onto a vertex. Then, it can describe only the relationship between a pixel and its neighborhood in a given radius.

III. PROPOSED APPROACH

This work proposes a method for IPDs classification using local and global approaches for texture description. To achieve this, we combine statistical and a new graph-based descriptors. Our proposal can be divided into three steps: The image to graph mapping process, the Feature extraction process, and finally, the classification process.

A. Mapping Images into Networks

Our first step is to model a grayscale image I into a network $G = (V, E)$ based on [8] and [9], where V is the set of all the vertices and E is the set of all edges. Each pixel $p_i = (x_{p_i}, y_{p_i})$ (where x and y represent its spatial position) has a intensity value associated $I(p_i) \in [0, 255]$. We map each p_i into a vertex (or node) $v_{p_i} \in V$.

We connect two vertices v_i and v_j if the Euclidean distance $d(p_i, p_j) = \sqrt{(x_{p_j} - x_{p_i})^2 + (y_{p_j} - y_{p_i})^2}$ is equal or less than a given radius r . For each graph edge $e \in E$, a weight e_{v_i, v_j} , defined by the value of the pixels intensity difference, is assigned, according Equation 1. Initially, this mapping is a regular weighted graph presenting connected vertices in a neighborhood defined by the radius r .

$$e_{v_i, v_j} = \begin{cases} I(p_i) - I(p_j), & \text{if } d(p_i, p_j) \leq r \\ NaN \text{ (Not a Number)}, & \text{otherwise} \end{cases} \quad (1)$$

In Equation 1, the non-existence of an edge is given by the Not a Number (*NaN*) symbol. Thus, to transform the obtained network into a complex network G , we applied a transformation $\phi(l, G)$, $\phi: G \rightarrow \mathcal{G}$ on the edges of the network to reveal the properties of the original image texture. It consists of selecting an edge according to the value of its weight e_{v_i, v_j} . Edges with weight less than a threshold l , are selected.

To obtain a directed graph, we discard links with negative weights. In Equation 2 we can see that edges with negative weights are excluded from the set of edges E . Therefore, the direction of an edge $e \in E$ in directed graph G is given by the pixel with larger intensity values to pixels with lower intensity values.

$$e_{v_j, v_i} = \begin{cases} e_{v_i, v_j}, & \text{if } 0 < e_{v_i, v_j} \leq l \\ NaN, & \text{otherwise} \end{cases} \quad (2)$$

We can see the transformation $\phi(l, G)$ as multiscale graph analysis, where \mathcal{G} is a multiscale graph set. For each value of l , the original graph is transformed into a l -scaled graph $G_l \in \mathcal{G}$. In this way, small values of l , provides detailed local information about image textures, while larger values of l presents better global information, such as image edges. We called l scaled threshold.

B. Features Extraction

As a global texture descriptor, we propose a new graph-based texture classification method using the Closeness Centrality metric. For a connected graph, we can see the *Closeness* of a vertex v_i a the inverse of the sums of the minimum path distances from v_i to all other vertices of the network. However, this definition is unsuitable when the network is disjointed, as some vertices are not reachable. Thus, a more common way to calculate the Closeness is from the sum of the inverses of the shortest path distances $CC(v_i) = \frac{1}{N-1} \sum_{j \neq i} \frac{1}{d_{v_i, v_j}}$, where, N is the number of vertices in the Graph; d_{v_i, v_j} is the length of the shortest path between two vertices v_i e v_j ; and $\frac{1}{d_{v_i, v_j}} = 0$ if there are no path between v_i and v_j .

Thus, the larger the value of *Closeness*, the more central the vertex. In general, the vertex with the highest value of *Closeness* has the best view of the information flow. Unlike [8], which uses input degree values of the network vertices, the *Closeness* can be seen as a global texture descriptor, since its value for each vertex is calculated considering all other vertices of the network.

Let D_l be the matrix of closeness values of the vertices $v_i \in V$ for a given threshold l . Every v_i has a corresponding $D_{l_i} \in D_l$, where $D_{l_i} = CC(v_i)$. We define the average degree matrix D as the average of D_l for all $l_i \in \{l_0, l_1, \dots, l_n\}$.

In this way, we propose the creation of a feature vector consisting of the relation between the intensity values of the image I and the values of the matrix D obtained by applying the centrality closeness measure over the graphs $G_l \in \mathcal{G}$. The value $d_i \in D$ is finally the average of all closeness values for all l -scaled graphs, for the vertex $v_i \in V$, and consequently, for the pixel $p_i \in I$. Figure 2 illustrates an example of the matrix D obtained from a set \mathcal{G} for $l = 10, 50, 150$.

If we take m intervals equally spaced in the intensity image range $[0, 255]$, we can call $[w_k, z_k]$ the k -th interval into the range. Then, the relation between the intensity values of the image I and the values of the matrix D can be expressed by $S_{w_k, z_k} = \sum_{d_i \in M} d_i$, where $M = \{d_i \in D | w_k \leq I(p_i) < z_k\}$. Then, for a single image, we finally obtain the feature vector $\mathcal{H}_G = \{S_{w_1, z_1}, S_{w_2, z_2}, \dots, S_{w_m, z_m}\}$.

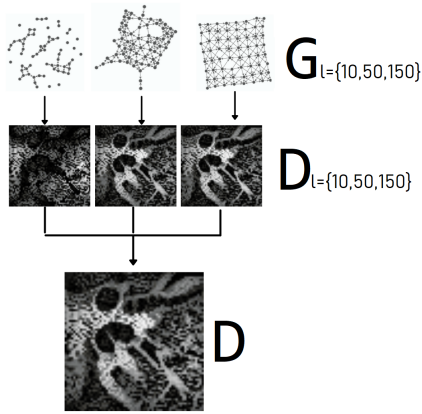


Fig. 2. From top to bottom: scaled graphs $G_l \in \mathcal{G}$ for $l = 10, 50, 150$, respectively; D_l obtained from the scaled graphs; and the final matrix D with the average of all closeness values for all l – scaled graphs.

As local texture descriptors, we applied two classical methods: Haralick [10] and LBP [11]. Haralick is a classical statistical method to represent image texture. In this paper, we used all 14 haralick descriptors proposed in [10]. LBP is a common and helpful method to describe texture. The LBP operator is its monotonic grayscale transformation invariance and its computational simplicity. We call these features obtained by haralick and LBP descriptors \mathcal{H}_e , and they were extracted from grayscale images.

The combined Feature vector is defined as $\mathcal{H} = [\mathcal{H}_G, \mathcal{H}_e]$. This is a graph-based and statistical representation of one image for the classification process.

C. Classification

To perform classification we chose the K-Nearest Neighbors (KNN) algorithm with *Minkowski* distance. We used this model because it is simple and, therefore, does not significantly influence the results. Consequently, using KNN gives more power to the feature vector obtained through the proposed method, since a more robust classification algorithm could affect the results.

IV. EXPERIMENTS AND RESULTS

We used a database containing 247 high-resolution Computed Tomography (CT) images presenting IPDs patterns to conduct this study. The images were selected by a group of radiologists, from 108 different exams performed at the Hospital das Clínicas, Faculty of Medicine of Ribeirão Preto, University of São Paulo (HCFMRP - USP) [12]. According to a radiology report, the images were grouped into six categories: honeycomb, ground glass, septal thickening, pulmonary consolidation, emphysematous areas, and healthy, with approximately 35 images per class. Examples of these ROIS can be see in Figure 1.

On Figure 3 we can see the algorithms performance as we increment l_0 and r . The values of $l_0 = 15$ and $l_0 = 35$ stand out once they present better accuracy, recall and precision when compared to other values. Given these metrics, we

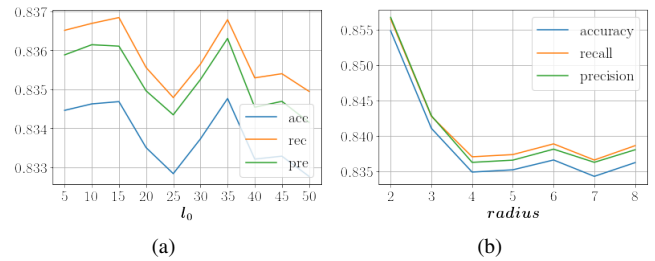


Fig. 3. (a) Initial threshold l_0 hyperparameter analysis. (b) Radius r hyperparameter analysis.

TABLE I
DIFFERENT METHODS' METRICS.

Method	Features	Acc.	Rec.	Prec.
GLCM	6	55.85%	56.09%	56.63%
LBP	10	51.01%	51.48%	51.56%
Haralick	14	79.28%	79.58%	79.61%
PCANet [5]	2048	81.35%	80.96%	82.33%
Proposed Approach	99	85.45%	85.62%	85.63%

Acc=Accuracy; Rec=Recall; Prec=Precision.

decided to run the experiments with $l_0 = 15$, once $l_0 = 35$ presents a peak along its neighborhood and can bring more uncertainty to the algorithm. We also used radius $r = 2$ to run the experiments once it presents the best metrics We believe that the smaller the radius, the better is for the method to detect variations in the images textures and, therefore, favoring the classification.

The threshold increment was defined as $l_i = 40$ and $m = 5$; For the vector S , we use 75 equally partitioned intervals that was normalized from $[0, 255]$ to $[0, 1]$. To generate the Statistical features we used the all 14 Haralick descriptors. For the Local Binary Pattern we set the radius as $r_{LBP} = 3$ and the number of points that define the circle around the pixel $n_{points} = 8 * r_{LBP} = 8 * 3 = 24$. In this way, we have a final vector \mathcal{H}_E of length = 99 capable of characterize the input image.

To perform classification, we executed the KNN algorithm 100 times with 5 neighbors and Minkowski distance. The experiments were executed in a notebook with Intel Core i5, 8GB memory RAM and operating system Linux Mint 20.1 Ulyssa.

A. Evaluation of the Proposed Approach

To analyse our method, we decided to extract 3 metrics from the evaluation step: accuracy, precision and recall. For the experiments, we used the Stratified K-Fold Validation method with a 10-fold split. Therefore, all the metrics were validated and presented on the tables using a mean of the algorithm's classification capability on each fold.

On Table I we can verify the performance of our approach when compared with different methods for texture classification problems, including the Machine Learning method proposed called PCANet [5]. We shows the performance metrics values and the number of extracted features of each

TABLE II
METRICS OF PROPOSED APPROACH BY PATTERN CLASS.

Class	Recall	Precision	F1-Score	Support
Healthy	88.60%	86.57%	87.57%	590
PC	87.10%	85.16%	86.12%	451
EA	90.11%	90.02%	90.06%	502
ST	73.69%	78.17%	75.86%	590
HC	85.25%	84.21%	84.73%	530
GGO	89.14%	88.76%	88.95%	595
Weighted AVG	85.48%	85.40%	85.42%	3258
Macro AVG	85.65%	85.48%	85.55%	3258

PC=Pulmonary Consolidation; EA=Emphysematous Area; ST=Septal Thickening; HC=Honeycomb; GGO= Ground-glass Opacity.

analysed method. Our proposed method surpassed the results of more classical methods from literature like GLCM, Local Binary Pattern (LBP) and Haralick. Our feature vector was capable of reaching better accuracy, recall and precision while increasing the number of features to 99.

Another way to analyse our proposed approach is to extract metrics for each IDP class. It is possible to be more precise about the algorithm's performance when dealing with these specific classes. For each class, we extracted recall, precision and f1-score. These metric values can be seen on Table II.

Emphysematous Area, Ground-glass opacity and Healthy are the classes with highest f1-score being 90.06%, 88.95% and 87.57%, respectively. The Pulmonary Consolidation class comes with, also, a higher than average f1-score of 86.12%. This means that, compared to the other classes, these four were better recognized by the algorithm. It is also important to notice the support for each class. Pulmonary Consolidation has only 451 cases on the dataset, which can affect the method's capacity of recognizing this specific class. Also, Emphysematous Area has the second lowest amount on the dataset with 502 occurrences, but was capable of having the highest precision, recall and f1-score out of all the classes. On the other hand, Septal Thickening got the most presence on the dataset with 590 occurrences but got the lowest f1-score of 75.86%, followed by Honeycomb with 84.73%.

On the bottom of Table II we displayed the same metrics for the proposed approach considering the weighted and macro average of all the classes. Our method got 85.55% and 85.42% of accuracy for macro and weighted average, respectively.

We can highlight the behaviour of the proposed method on the context of three classes: Healthy, Ground-glass Opacity and Pulmonary Consolidation. These metrics represent a relevance of the method on the problem of diagnosing cases of COVID-19 once Ground-glass Opacity and Pulmonary Consolidation are abnormalities present on computed tomography of patients that contracted the disease [13]. Therefore, it is suggested that the proposed approach can be of great importance on the aid of diagnosing patients suspected to have been infected with COVID-19.

V. CONCLUSION

This work presented an approach that extracts texture characteristics from High resolution tomography images with IPDs. The proposed method combines graph-based and statistical texture descriptors (Haralick and LBP) to classify the images into five different types of Interstitial Pulmonary Diseases (IPDs). We map the original into directed complex networks. Each pixel was considered as a vertex of the network connecting vertices within a given radius. We extract the centrality measure closeness from multiple scaled networks, and a vector of texture features is formed from the sum of the closeness values within a specific interval. We compared our proposal with traditional methods of texture classification. The increase in performance of our method overcomes the traditional approaches. Thus, it is stated that the proposed method has great representation in the extraction of texture features from images with IPDs, which are diseases that have a consistently bad rating. It is essential to observe that our proposed method presents better performance results for IPDs patterns of Pulmonary Consolidation and Ground-glass Opacity, typically found in COVID-19 patients.

REFERENCES

- [1] L. C. Pereyra, R. M. Rangayyan, M. Ponciano-Silva, and P. M. Azevedo-Marques, "Fractal analysis for computer-aided diagnosis of diffuse pulmonary diseases in HRCT images," *IEEE MeMeA 2014 - IEEE International Symposium on Medical Measurements and Applications, Proceedings*, 2014.
- [2] K. Mori, "Chapter 4 - cad in lung," in *Handbook of Medical Image Computing and Computer Assisted Intervention*, ser. The Elsevier and MICCAI Society Book Series, S. K. Zhou, D. Rueckert, and G. Fichtinger, Eds. Academic Press, 2020, pp. 91–107. [Online]. Available: <https://www.sciencedirect.com/science/article/pii/B9780128161760000090>
- [3] W. N. Goncalves, A. R. Backes, A. S. Martinez, and O. M. Bruno, "Texture descriptor based on partially self-avoiding deterministic walker on networks," *EXPERT SYSTEMS WITH APPLICATIONS*, vol. 39, no. 15, pp. 11 818–11 829, NOV 1 2012.
- [4] J. J. J. de Mesquita Sa, A. R. Backes, and P. C. Cortez, "Texture analysis and classification using shortest paths in graphs," *PATTERN RECOGNITION LETTERS*, vol. 34, no. 11, pp. 1314–1319, AUG 1 2013.
- [5] T.-H. Chan, K. Jia, S. Gao, J. Lu, Z. Zeng, and Y. Ma, "PCANet: A Simple Deep Learning Baseline for Image Classification?" *IEEE TRANSACTIONS ON IMAGE PROCESSING*, vol. 24, no. 12, pp. 5017–5032, DEC 2015.
- [6] R. S. Cabral, A. C. Frery, and J. A. Ramirez, "Variability analysis of complex networks measures based on stochastic distances," *PHYSICA A-STATISTICAL MECHANICS AND ITS APPLICATIONS*, vol. 415, pp. 73–86, DEC 1 2014.
- [7] P. Simon and V. Uma, "Review of Texture Descriptors for Texture Classification," *Data Engineering and Intelligent Computing, Advances in Intelligent Systems and Computing 542.*, vol. 542, pp. 159–176, 2018.
- [8] W. N. Gonçalves, N. R. da Silva, L. da Fontoura Costa, and O. M. Bruno, "Texture recognition based on diffusion in networks," *Inf. Sci.*, no. C, p. 51–71, Oct. 2016. [Online]. Available: <https://doi.org/10.1016/j.ins.2016.04.052>
- [9] L. N. Couto, A. R. Backes, and C. A. Barcelos, "Texture characterization via deterministic walks' direction histogram applied to a complex network-based image transformation," *Pattern Recognition Letters*, vol. 97, pp. 77–83, 2017. [Online]. Available: <https://www.sciencedirect.com/science/article/pii/S0167865517302453>
- [10] R. HARALICK, K. SHANMUGAM, and I. DINSTEN, "TEXTURAL FEATURES FOR IMAGE CLASSIFICATION," *IEEE TRANSACTIONS ON SYSTEMS MAN AND CYBERNETICS*, vol. SMC3, no. 6, pp. 610–621, 1973.

- [11] T. Ojala, M. Pietikainen, and D. Harwood, "A comparative study of texture measures with classification based on feature distributions," *PATTERN RECOGNITION*, vol. 29, no. 1, pp. 51–59, JAN 1996.
- [12] L. C. Pereyra, R. M. Rangayyan, M. Ponciano-Silva, and P. M. Azevedo-Marques, "Fractal analysis for computer-aided diagnosis of diffuse pulmonary diseases in hrct images," in *2014 IEEE International Symposium on Medical Measurements and Applications (MeMeA)*, 2014, pp. 1–6.
- [13] X. He, J. Zheng, J. L. Ren, G. Zheng, and L. Liu, "Chest high-resolution computed tomography imaging findings of coronavirus disease 2019 (Covid-19) pneumonia," *INTERNATIONAL JOURNAL OF RADIATION RESEARCH*, vol. 18, no. 2, pp. 343–349, APR 2020.